Real-time Identification of Electromechanical Oscillations through Dynamic Mode Decomposition

Alberto Berizzi[1], Alessandro Bosisio[1], Riccardo Simone[1], Andrea Vicario[1]
Giorgio Giannuzzi[2], Cosimo Pisani[2], Roberto Zaottini[2]

[1] Department of Energy, Politecnico di Milano, Via la Masa 34, Milano, Italy
[2] Terna S.p.a., Via Egidio Galbani 70, Roma, Italy

Abstract: the increasing penetration of inverter-based resources is affecting the overall power system security, so that effective tools are needed to provide system awareness and identify the most suited countermeasures. To tackle this problem, real-time monitoring and assessment of transmission grids based on synchrophasor measurements have drawn the attention of many researchers over the last decade, thanks to the high temporal resolution of data provided by Phasor Measurement Units (PMUs). In this paper, a new version of the Dynamic Mode Decomposition (DMD) is proposed as a tool for the real-time identification of electromechanical oscillations. This approach is able to provide information on the dynamic characteristics (frequency and damping) and the spatial correlation (mode shape) of the modes identified. Besides, an improved criterion is used to track and discern the dominant modes. The effectiveness of the DMD method has been tested on the two-area Kundur system and validated using data from a real event on the European synchronous grid, giving promising results. Thanks to its reliability and robustness, the DMD is now implemented in the Terna (the Italian TSO) Wide Area Measurement System (WAMS) in use in the control room.

1. Introduction

The recent development of Wide Area Measurements Systems (WAMS) using Phasor Measurement Units (PMUs) is arising the interest of Transmission System Operators (TSOs) on new techniques for real-time power system monitoring. Among others, real-time identification of electromechanical oscillation modes using streaming data has gained attention due to the ever-increasing installation of inverter-based resources, that are reducing the overall system inertia, leading to possible critical system operation and low damping conditions.

Electromechanical oscillations have been deeply investigated in the past using small perturbation stability analysis [1]. Such oscillations (typically between 0.1 Hz and 2 Hz), can be classified either as local modes or as interarea modes. Interarea oscillations are of particular interest for TSOs; they can be either very low frequency modes (0.1-0.3 Hz), involving all the system generators, or higher frequency modes (0.4-0.7 Hz), involving groups of generators. A further type of oscillations is known as forced oscillations, caused by external driving forces (typically malfunctioning controllers or failures) [2], [3]. Such types of oscillations can be avoided by a careful maintenance of generation controls and never appeared so far in Europe.

Small-perturbation analysis based on modelling is carried out linearizing the system around an operation point. This kind of analysis is very challenging for a real-time application in terms of computational time and data availability: hence, an efficient and fast algorithm is necessary in that framework.

On the one hand, different methods, called Linear Ringdown Analysis, like the Eigensystem Realization Algorithm (ERA) [4], later re-adapted and improved in [5], the Prony Method [6] or the Pencil Method [7], have already been used to analyse data streams coming from transient events.

However, subspace identification methods are the most promising techniques. These approaches offer significant performances and the advantage to be resilient to the unavailability or corruption of real-time measurements, giving a sort of "filtered synthesis" of the information processed. Authors in [8] use the Canonical Correlation Analysis subspace to identify frequency and damping for the Brazilian system. In [9] a recursive stochastic subspace identification is applied, while in [10] a Fast Frequency Domain Decomposition (FDD) is used. An enhanced Kalman filter has been applied in [11]: however inadequate initial conditions may result in convergence errors or biased results. Another method considers vector fitting, where oscillatory modes are estimated in the frequency domain from a post-disturbance ringdown response [12]. In [13] the estimation of the dynamic matrix of the system is used to detect critical oscillations. Nevertheless, the proposed methodology was not tested using real PMU data.

Authors in [14] tackle the issue of electromechanical mode identification through a measurement-based methodology employing a novel signal decomposition theorem based upon the Hilbert transform. This method has been improved in [15], where a different non-linear least squares method for estimating the damping levels of real-life electromechanical oscillations in power systems is presented.

An alternative method, recently developed, focuses on the identification of electromechanical oscillations exploiting the Principal Component Analysis (PCA) applied to PMU data; frequency and damping are further identified by Prony analysis [16] and also approximated information about mode shapes are determined. PCA is also used in [17], where PMU data are dimensionally reduced and analysed by an Artificial Neural Network.

Finally, [18] investigates on the dynamic response of a grid-tied Voltage Source Converter during electromechanical oscillations, using the Adaptive Local

Iterative Filter Decomposition presented by [19] to identify oscillation parameters.

This paper presents a PMU-based method for the characterization of electromechanical oscillations, based on the Dynamic Mode Decomposition (DMD). Originally proposed in [20], and applied to power systems in [21], [22], the DMD has the advantage, over most of the above mentioned techniques, that it can identify frequency, damping and spatial correlations (mode shapes) of the oscillations. A different version of the DMD is used in [23] for the extraction of electromechanical oscillations from a noisy data set; however, its computation time is in general significantly higher than the original algorithm.

Different from previous papers, in this work a new DMD formulation based on [24] is deeply investigated, where the DMD (*exact DMD*) is defined by the eigendecomposition of an approximating linear operator. This new definition has been recognized of paramount importance, since it allows considering the DMD as an approximation of the Koopman spectral analysis. The Koopman operator is indeed a linear, infinite-dimensional, operator, whose modes and eigenvalues capture the evolution of observables describing any dynamical system. Whereas previous DMD theory focuses on full-rank, sequential time series, this approach applies more generally to pairs of n-dimensional data vectors (x_{k+1} and x_k) and can hence be used with a wider class of data sets, even rank-deficient. It can also be demonstrated that the DMD is closely-related to the ERA algorithm: the latter is often applied to experimental data where the underlying system may be approximately linear, while the DMD is designed to analyse any dynamical system [24], even large and nonlinear, like power systems are.

A second original contribution of this paper is related to monitoring: it is very important to issue alarms when oscillations are becoming dangerous. In this paper, alarms are based on a new index, i.e., a pseudo-energy: while previous methods based on DMD classify each identified mode according to the mode norm, in this paper the mode evolution within the whole sampling space is also taken into account, providing a more accurate ranking of dominant modes [25], whatever the system order or the size of the data analysed.

In order to assess its performance, the accuracy and stability of the proposed algorithm has been first assessed on a test system whose analytical model is well known. According to the experience gained on the test system, the algorithm has been then implemented in the WAMS testing environment of Terna (the Italian TSO) which also receives data from several TSOs related to the European continental power systems. It is performing very well, proving to be very little sensitive to noise, thanks to the different pseudo-energy proposed here to track the dominant modes. This peculiarity has been proved to be robust to handle false alarms, in comparison to other methods previously tested.

The remaining of this paper is organized as follows: Section 2 presents the DMD algorithm with reference to the identification of electromechanical oscillations. Section 3 reports the results of the application of the proposed approach on both the Kundur two-area test system, using different sets of measurements, including non-state variables, and European grid frequencies. Conclusions are provided in Section 4.

2. The Dynamic Mode Decomposition

The DMD was originally proposed to extract dynamic information from experimental data of field flows [20]. Kutz et al. [24] provided the most modern definition of the method, sometimes known as *exact DMD*, achieved by a similarity transformation of the system matrix; it is considered numerically more stable and robust [25].

2.1. The DMD architecture

In the DMD architecture, data are collected from a dynamical system:

$$\frac{dx}{dt} = f(\boldsymbol{x}, t, \boldsymbol{\mu}) \tag{1}$$

where $\boldsymbol{x}(\boldsymbol{t}) \in \mathbb{R}^n$ is a vector representing the state of the dynamical system at time t, vector $\boldsymbol{\mu}$ contains the parameters of the system and $f(\cdot)$ represents its dynamics. The continuous-time dynamics (1) may be described by the discrete-time representation, where the system is sampled every Δt (giving n spatial measurements for m time snapshots), so that:

$$\boldsymbol{x}_k = \boldsymbol{x}(k\Delta t) \tag{2}$$

Denoting the discrete-time flow map obtained by evolving (1) for Δt by F:

$$\boldsymbol{x}_{k+1} = F(\boldsymbol{x}_k) \tag{3}$$

the n measurements y are taken by the system at time t_k, where $k = 1,2,\dots,m$:

$$\boldsymbol{y}_k = g(\boldsymbol{x}_k) \tag{4}$$

In some applications, as a particular case, the measurements are the state variables, so that:

$$\boldsymbol{y}_k = \boldsymbol{x}_k \tag{5}$$

Initial conditions are described by the vector:

$$\boldsymbol{x}(0) = \boldsymbol{x}_1 \tag{6}$$

In general, it is not possible to find out the analytic solution to nonlinear equations (1), and numerical solutions are used to evolve to future states. The DMD takes an equation-free perspective, where the dynamics $f(\boldsymbol{x}, t, \boldsymbol{\mu})$ are often unknown: data from measurements are used to approximate the dynamics with locally linear systems:

$$\frac{dx}{dt} = \mathbf{A}\mathbf{x} \tag{7}$$

with initial condition $\boldsymbol{x}(0)$:

$$\boldsymbol{x}(t) = \sum_{j=1}^{n} \boldsymbol{\phi}_j \exp(\omega_j t)\, b_j = \boldsymbol{\Phi}\exp(\boldsymbol{\Omega} t)\boldsymbol{b} \tag{8}$$

where $\boldsymbol{\phi}_j$ and ω_j are the eigenvectors and eigenvalues of the matrix $\mathbf{A}$, and coefficient b_j are the coordinates of $\boldsymbol{x}(0)$ in the eigenvector basis. Discretising equation (7) with sampling time Δt, it is possible to write:

$$\mathbf{x}_{k+1} = \mathbf{B}\mathbf{x}_k \tag{9}$$

where:

$$\mathbf{B}=\exp(\mathbf{A}\Delta t) \tag{10}$$

Matrices $\mathbf{A}$ and $\mathbf{B}$ are linked by the following property: they have the same eigenvectors $\boldsymbol{\phi}_j$ and their eigenvalues are such that $\lambda_k = e^{\omega_k \Delta t}$, where λ_k is the *k-th* eigenvalue of B. The solution to (10) can be approximated by a reduced (r) set of eigenvalues λ_k (hold in the diagonal matrix $\boldsymbol{\Lambda_r}$) and reduced eigenvector matrix $\boldsymbol{\Phi_r}$ of $\mathbf{B}$:

$$\mathbf{x}_{k+1} \approx \sum_{j=1}^{r} \boldsymbol{\phi}_j \lambda_j^k b_{rj} = \boldsymbol{\Phi_r}\boldsymbol{\Lambda_r^k}\mathbf{b_r} \tag{11}$$

where $\mathbf{b_r}$ are the coefficients of the initial condition $\mathbf{x}_1$ in the eigenvector basis so that $\mathbf{x}_1 = \boldsymbol{\Phi_r b_r}$. In other terms, the DMD performs a low-rank eigendecomposition of $\mathbf{B}$ that optimally fits the measured data. Moreover, the DMD approximates the dynamics of the nonlinear system in a least-squares sense (L_2 *norm*): the matrix $\mathbf{B}$ indeed optimally fits the measured trajectory x_k for $k = 1,2,\dots,m$ so that:

$$\|\mathbf{x}_{k+1} - \mathbf{B}\mathbf{x}_k\|_2 \tag{12}$$

is minimized across all points for $k = 1,2,\dots,m-1$.

2.2. Characterizing the DMD algorithm

The approximation above described holds only over the sampling window where $\mathbf{B}$ is built in (9). The approximated solution can be used both to make future state predictions and to decompose the dynamics into various time scales, since λ_k are specified. To minimize the error (12) across all snapshots $k = 1,2,\dots,m$, it is possible to arrange the m snapshots into two large data matrices:

$$\mathbf{X} = \begin{bmatrix} | & | & \cdots & | \\ \mathbf{x}_1 & \mathbf{x}_2 & \cdots & \mathbf{x}_{m-1} \\ | & | & \cdots & | \end{bmatrix} \tag{13}$$

$$\mathbf{X}' = \begin{bmatrix} | & | & \cdots & | \\ \mathbf{x}_2 & \mathbf{x}_3 & \cdots & \mathbf{x}_m \\ | & | & \cdots & | \end{bmatrix} \tag{14}$$

It is then possible to rewrite (9) as follows:

$$\mathbf{X}' = \mathbf{B}\mathbf{X} \tag{15}$$

Hence, the best-fit matrix ($\mathbf{B}$) is given by:

$$\mathbf{B} = \mathbf{X}'\mathbf{X}^{\dagger} \tag{16}$$

where † represents the Moore-Penrose pseudoinverse [26]. Consider the Singular Value Decomposition (SVD) of $\mathbf{X}$:

$$\mathbf{X} = \mathbf{U}\boldsymbol{\Sigma}\boldsymbol{V}^* \tag{17}$$

where $\boldsymbol{\Sigma}$ is a nxm matrix containing the Singular Values (SV), $\mathbf{U}$ (a nxn matrix) and $\mathbf{V}$ (a mxm matrix) are orthonormal matrices containing in rows the left and right singular vectors respectively, and $*$ denotes the conjugate transpose. The solution minimizing the error in (12) is given by the pseudoinverse:

$$\mathbf{X}^{\dagger} = \mathbf{V}\boldsymbol{\Sigma}^{-1}\mathbf{U}^* \tag{18}$$

When the size of the system n is large, the use of $\mathbf{B}$ may be challenging and it would be computationally expensive to eigendecompose it directly. Hence, the DMD algorithm computes a rank reduced representation in terms of a Proper Orthogonal Decomposition (POD) projected matrix $\widetilde{\mathbf{B}}$. The SVD is characterized by important properties: the left singular values $\mathbf{U}$ are the POD modes and contain the spatial correlations in the data, while temporal information is found in $\mathbf{V}$. Rank truncation is performed in order to reduce the dimension of the system. If low-dimensional structure is present in the data, the SV in $\boldsymbol{\Sigma}$ will decrease sharply to zero with only a limited number r of dominant modes.

The data matrix can be approximated by:

$$\mathbf{X} \approx \mathbf{U}_{\mathrm{r}}\boldsymbol{\Sigma}_{\mathrm{r}}\mathbf{V}_{\mathrm{r}}^* \tag{19}$$

Where $\mathbf{U_r}$ has dimensions nxr, $\boldsymbol{\Sigma_r}$ rxr and $\mathbf{V_r}$ mxr, and r is the rank of the reduced SVD approximation of $\mathbf{X}$. Matrix $\mathbf{B}$ can be obtained by substituting (19) into (16):

$$\mathbf{B} = \mathbf{X}'\mathbf{V}_{\mathrm{r}}\boldsymbol{\Sigma}_r^{-1}\mathbf{U}_{\mathrm{r}}^* \tag{20}$$

and, more efficiently, projecting $\mathbf{B}$ into the POD modes, an upper triangular matrix $\widetilde{\mathbf{B}}$ is obtained:

$$\widetilde{\mathbf{B}} = \mathbf{U}_{\mathrm{r}}^*(\mathbf{X}'\mathbf{V}_{\mathrm{r}}\boldsymbol{\Sigma}_r^{-1}\mathbf{U}_{\mathrm{r}}^*)\mathbf{U}_{\mathrm{r}} = \mathbf{U}_{\mathrm{r}}^*\mathbf{X}'\mathbf{V}_{\mathrm{r}}\boldsymbol{\Sigma}_{\mathrm{r}}^{-1} \tag{21}$$

$\widetilde{\mathbf{B}}$ defines a low-dimensional linear model of the dynamical system on POD coordinates (that can be used for the approximation (11)), such that:

$$\tilde{\mathbf{x}}_{k+1} = \widetilde{\mathbf{B}}\tilde{\mathbf{x}}_k \tag{22}$$

2.3. Identification of the mode properties

In order to identify the mode properties, frequencies, dampings and the mode shapes, it is necessary to reconstruct the high-dimensional state $\boldsymbol{x}_k \approx \boldsymbol{U}\tilde{\boldsymbol{x}}_k$ and solve the eigenvalue problem for $\widetilde{\mathbf{B}}$:

$$\widetilde{\mathbf{B}}\mathbf{W} = \mathbf{W}\boldsymbol{\Lambda_r} \tag{23}$$

where the columns of $\mathbf{W}$ (rxr) are the eigenvectors and $\boldsymbol{\Lambda_r}$ is a diagonal matrix (rxr) containing the eigenvalues λ_j of $\widetilde{\mathbf{B}}$, a subset of the eigenvalues of $\mathbf{B}$. Finally, it is possible to reconstruct the eigendecomposition of $\mathbf{B}$ from $\mathbf{W}$ and $\boldsymbol{\Lambda_r}$. A subset of the eigenvalues of $\mathbf{B}$ are given by $\boldsymbol{\Lambda_r}$, while a subset of the eigenvectors $\boldsymbol{\phi}_j$ are given by the columns of $\boldsymbol{\Phi_r}$:

$$\boldsymbol{\Phi_r} = \mathbf{X}'\mathbf{V}_{\mathrm{r}}\boldsymbol{\Sigma}_{\mathrm{r}}^{-1}\mathbf{W} \tag{24}$$

Columns of $\boldsymbol{\Phi_r}$ are defined as "exact DMD modes". In the original DMD formulation [20], the DMD modes are computed as:

$$\boldsymbol{\phi_r} = \mathbf{U}_{\mathrm{r}}\mathbf{W} \tag{25}$$

and defined as "projected DMD" modes, since, as demonstrated in [24], they are not the eigenvectors of the approximating linear operator. The two formulations in (24) and (25) tend to converge if $\mathbf{X}$ and $\mathbf{X}'$ have the same column spaces.

Finally, the approximated solution for all future times is given by:

$$\mathbf{x}(t) \approx \sum_{j=1}^{r} \boldsymbol{\phi}_j \exp(\omega_j t)\, b_{rj} = \boldsymbol{\Phi_r}\exp(\boldsymbol{\Omega_r} t)\mathbf{b_r} \tag{26}$$

where $\omega_j = \ln(\lambda_j)/\Delta t$ are eigenvalues of $\mathbf{A}$ in the time domain, $\mathbf{b_r}$ is a vector whose entries are the initial amplitudes b_{rj} of each mode, $\boldsymbol{\phi}_j$ is the DMD eigenvector of each mode, $\boldsymbol{\Omega_r}$ is a diagonal matrix whose entries are a subset of the eigenvalues ω_j. The amplitude of a given DMD mode ($\mathbf{b_r}$) may be interpreted as the power spectrum given by the Fast Fourier Transform (FFT) [27].

It is possible to compute the initial amplitudes b_{rj} of the modes, by considering the first snapshot $\mathbf{x}_1$ at $t = 0$ in (26):

$$\mathbf{x}_1 \approx \boldsymbol{\Phi_r}\mathbf{b_r} \tag{27}$$

Since $\boldsymbol{\Phi_r}$ is generally a non-square matrix, the vector of initial amplitudes is computed by using the pseudo-inverse, equivalent to finding the best-fit solution $\mathbf{b_r}$, in the least-squares sense:

$$\mathbf{b_r} = \boldsymbol{\Phi_r}^{\dagger}\mathbf{x}_1 \tag{28}$$

Frequency f and damping ratio ξ of the identified modes are finally computed from the eigenvalues ($\omega_j = \alpha \pm j\beta$), while the mode shapes of the measurements are given by the columns of (24).

$$f = \frac{\beta}{2\pi} \tag{29}$$

$$\xi = \frac{-\alpha}{\sqrt{\alpha^2+\beta^2}} \quad (30)$$

2.4. *Connection with the Koopman analysis*

In the standard DMD, measurements of the system states are taken to build a model that maps $\boldsymbol{X}$ to $\boldsymbol{X}'$. Nevertheless, the DMD can also be applied to the space of observables, which are commonly more accessible.

Kutz et al., [27], demonstrated that DMD is strongly connected to the Koopman spectral theory. The Koopman spectral analysis augments the measurements with the non-linear observations $\boldsymbol{y} = \boldsymbol{g}(\boldsymbol{x})$ to provide a mapping between $\boldsymbol{Y}$ and $\boldsymbol{Y}'$, the matrices of the observables. The Koopman operator, introduced by [28], is an infinite-dimensional linear operator, which describes how measurements of dynamical system evolve through the nonlinear dynamics.

The described algorithm can be hence used to produce $\boldsymbol{A_Y} = \boldsymbol{Y}'\boldsymbol{Y}^{\dagger}$ and to apply the DMD on the space of observables instead of the state-space.

2.5. Selection of the dominant modes

The DMD can extract the most important spatio-temporal patterns and eigenvalues from a data set, but the ranking of the modes is not unique. Therefore, it is necessary to find out a criterion to select the most significant modes and the related transient. For this goal, it is possible to associate each eigenvalue/mode with a pseudo-energy. For example, in [21] the energy of each mode is taken from a method that resembles an SVD/POD-based approach. Another way is given by [8], while a possible formula for a pseudo-energy is defined in [29]. In this paper, a different approach based on [25] is used to rank the identified modes and identify the dominant ones. For each mode *j*, the energy E_j of the DMD mode is computed:

$$E_j = \left| b_{rj} e^{\omega_j \mathrm{T}} \right| \quad (31)$$

where *T* is the whole-time frame analysed. This expression has the advantage that the evaluation of the energy is hence not limited to a single point in time, but it is extended to the whole window.

Modes are then ranked according to the energy and those with the largest values are assumed to be the dominant. As reported in [8] and confirmed by the simulations, DMD modes related to physical modes have higher energy than spurious modes, with almost the same damping and frequency for different system orders and with different size of the time window analysed.

3. Tests and results

The DMD algorithm has been initially tested on the two-area Kundur system [1], for comparison with the traditional modal analysis, to assess its ability and accuracy. In particular:

- both a fixed time window and sliding windows have been considered;
- to test the DMD sensitivity, heterogeneous types of data, acquired from PMU placed on the busbars, have been employed.

The DMD algorithm goes as follows:

A. data are stacked in two matrices, **X** and **X'** of (13) and (14), where each row contains data from a PMU and the columns contain data samples;
B. the reduced order matrix $\widetilde{\mathbf{B}}$ is computed by (21);
C. the eigenvalue problem (23) is solved;
D. the relative energy is computed (31).

Finally, for significant modes, frequency (29), damping (30) and mode shapes (24) are provided and results are compared with the standard Small-Perturbation Angle Stability analysis (SPAS).

Since the DMD approximates the dynamics of the nonlinear dynamical system in a least-squares sense, to minimize the error in (12), spurious modes may appear to fully approximate the samples available. In order to extract only physically meaningful modes, these spurious modes are discarded based on their pseudo-energy.

Eventually, the proposed DMD algorithm has been implemented in the Terna WAMS testing environment and it is currently running on-line for the monitoring of oscillatory instability of the Italian system in its interconnected operation with the Continental European power system. It is worth noticing that Terna is equipped with one of the largest WAMS worldwide, including more than internal 150 PMUs providing data in real-time and exchanging data with several European TSOs. The efficiency of the proposed method in the real-time environment (including all problems related to noise, filtering, etc.) is proved with reference to a real event, occurred in the European Synchronous grid, that resulted in interarea oscillations.

3.1. Kundur Test system

The Kundur two-area test system [1] is shown in Fig. 1.

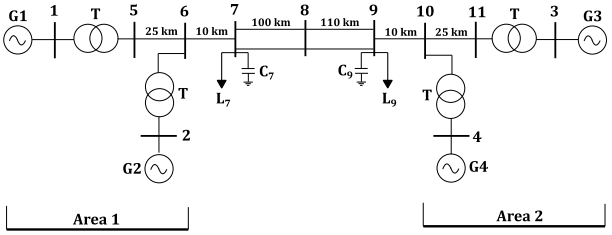

Fig. 1. *Kundur two-area test system [1].*

It is made by 11 buses and two parallel tie lines connecting the two areas. Generators are modelled with the 6th order model, and equipped with Automatic Voltage Regulators, speed governors and Power System Stabilizers.

The SPAS analysis identifies three electromechanical modes:

- a local mode associated to Area 1, with frequency 1.07 Hz and damping ratio 0.12;
- a local mode associated to Area 2, with frequency 1.13 Hz and damping ratio 0.19;
- an inter-area mode, with frequency 0.56 Hz and damping ratio 0.05.

The mode shape of the inter-area mode is reported in Fig. 2:

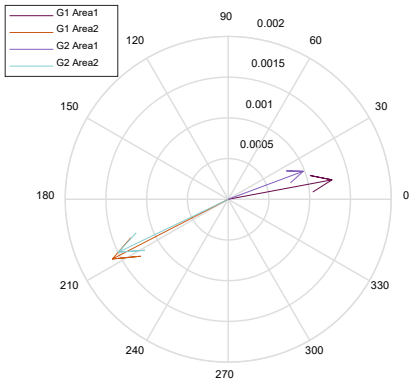

Fig. 2. *Mode shape associated to the inter-area mode.*

In order to trigger an inter-area event, an equal, opposite and simultaneous torque variation (±15%) in two generators (G2 and G4) is applied [30]. The proposed method has been tested considering the availability of the following variables, sampled at 500Hz (2ms): the speed of each generator, the frequency from each bus, the real power flow on each line.

According to [31], data have been normalized by mean removal; no further filtering has been applied.

3.1.1. Simulation results considering multiple inputs

As a first case, all available data are used by the DMD with a fixed time window of 15s.

Fig. 3 shows that the SVs above the $5^{th}/6^{th}$ component are very close to zero. Hence, rank truncation has been applied with $r = 6$. In general, truncating the system enables to filter noise of measurements from the energy of the modes. It is usually possible to increase the amount of data until the system reaches full rank numerically. However, if the system is already numerically full rank, adding more signals will result only in the appearance of new SVs and spurious DMD high frequency modes [27].

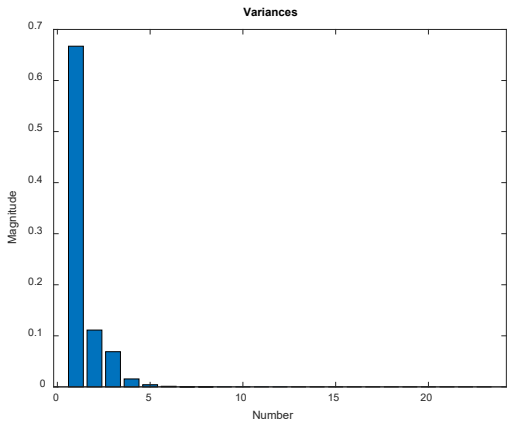

Fig. 3. *Variances of the measurements analysed.*

Fig. 4 shows the power spectrum associated to all frequency measurements, where a peak at 0.52 Hz is shown.

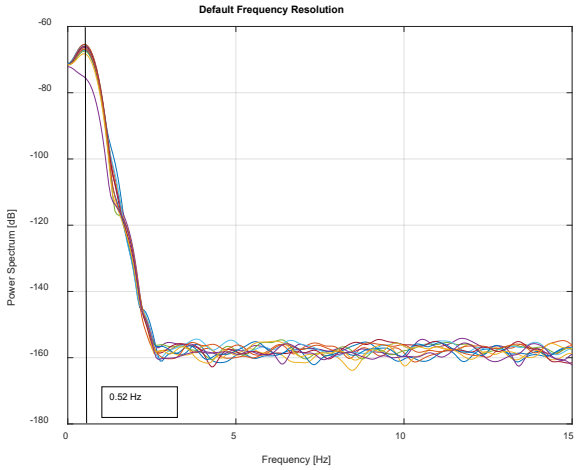

Fig. 4. *Power spectrum.*

Results of the DMD are given in Table 1, where modes are ranked based on their energy. The most energetic mode, at 0.51 Hz, is clearly identified; its damping is also estimated with great accuracy. The second and third modes are spurious modes, characterized by lower energy content.

Table 1 *Frequency, damping and relative energy of the identified modes.*

Mode	*f [Hz]*	ξ	$E_{\%}$	λ
1	0.51	0.04	33.677	-0.1 ± j3.2
2	0.09	0.56	12.981	-0.4 ± j0.6
3	0.73	0.17	3.341	-0.8 ± j4.6

To validate the results, the estimated mode shapes have to be considered as well. Fig. 5 shows a comparison of the speed mode shapes of the inter-area mode given by SPAS (left) and the first energetic mode identified by the DMD (right). Values of SPAS have been normalized to appreciate the graphical similarity. It is worth noticing that the inter-area mode shape is identified with very good accuracy, proving that the pseudo energy criterion works well.

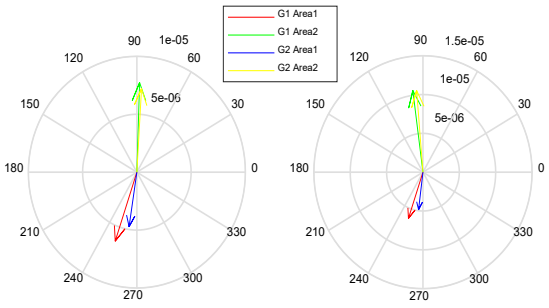

Fig. 5. *Mode shapes comparison.*

The same data have been analysed with a smaller size sliding windows to emulate the analysis of streaming data. For example, the results relevant to a 2.5 seconds sliding window are shown in Fig. 6, proving that the proposed method can be used in real-time to track interarea modes.

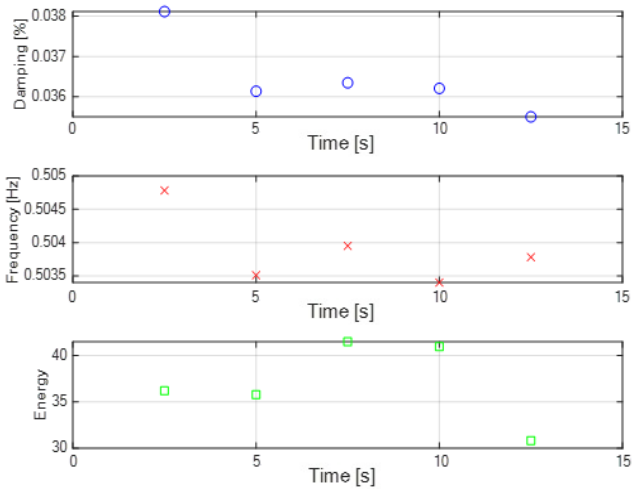

Fig. 6. *Frequency, damping and absolute energy of the most energetic oscillatory mode in each time window analysed.*

It is worth noticing that frequency and damping estimations tend to fluctuate, but they remain close to the exact values. The energy shows little fluctuations as well.

3.1.2. Simulation results considering the busbars frequency

In order to investigate the behaviour of the proposed method depending on the measurements considered, only the frequencies of the 11 busbars are hereinafter considered as input, assuming that speed measurements are not available for the TSO. Under this assumption, the mode shapes given by the DMD are no longer comparable with the SPAS, since the latter only provides results associated to state variables.

A fixed time window of 15 seconds has been considered, rank has been set to 9 and data have been normalized by mean removal. Fig. 7 shows the 11 normalized frequencies analysed.

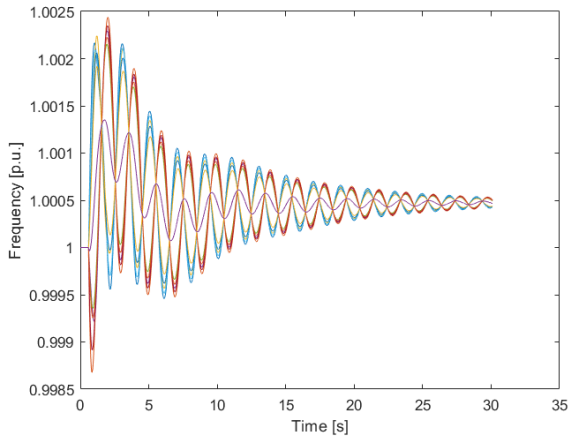

Fig. 7. *Normalized frequencies of the 11 busbars.*

Features of the identified DMD modes are shown in Table 2.

Table 2 *Frequency, damping and relative energy of the modes considered.*

Mode	*f [Hz]*	*ξ*	$E_{\%}$	*λ*
1	0.50	0.10	40.748	-0.3 ± j3.2
2	0	1	14.179	-0.2
3	0.62	0.63	1.562	-3.2 ± j3.9
4	0.98	0.13	0.559	-0.8 ± j6.2
5	0	1	0.057	2483.3
6	0	1	0.016	1626.2

The algorithm identifies few oscillatory modes: the frequency of most energetic one, at 0.50 Hz, is close to the "exact" inter-area mode and detected by the spectral analysis of Fig. 4. Again, the remaining modes are to be considered as spurious and they have, at any rate, very low energy.

The knowledge of the mode shapes related to the most energetic DMD mode is extremely useful for the system operator, as it gives a physical interpretation of the ongoing oscillation, as Fig. 8 depicts.

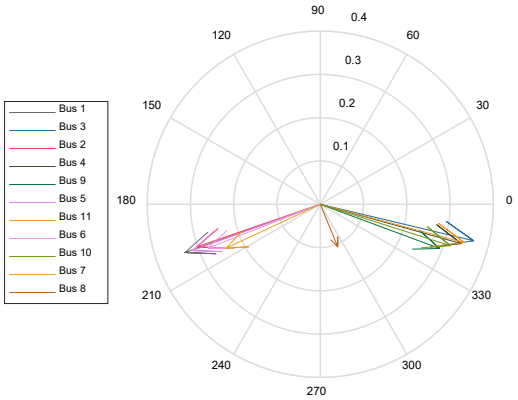

Fig. 8. *Mode shape associated to the most energetic mode.*

Fig.8 clearly shows that the frequency of buses 1-2-5-6-7 in Area 1 swing against the frequency of buses 3-4-9-10-11 in Area 2 while bus 8 is, as expected, unaffected. Mode shapes of the other identified modes are not shown, as they are related to low-energy modes.

The selected results shown here have been used to tune parameters for the real-time application of the proposed algorithm in the security monitoring system of Terna. The studies carried out on the test system prove that the proposed algorithm is suitable for the characterization of interarea modes using only frequency measurements. Moreover, the estimation of damping was also found to be very satisfactory for the monitoring of security, as well as mode shapes.

3.2. Real-time application to the European Synchronous grid

In this section, some results of the application of the proposed DMD approach to the Continental European grid operation are presented. The Continental European power system interconnects 24 European Countries. Based on ENTSO-E reports and on the experience of involved TSOs

over the years, it is possible to identify the most typical electromechanical modes of the European grid (Fig. 9):

Fig. 9. *Most dominant modes of the European grid.*

- a N-S mode with frequency 0.3 Hz;
- two E-W modes with frequencies 0.15 Hz and 0.20 Hz;
- a dominant global mode that may have three different values of frequency: 0.15 Hz, 0.20 Hz or 0.30 Hz.

In the past 10 years, Terna tested, for its real-time monitoring system, many different approaches (e.g., PCA combined with Prony [16] and FDD [10], as well as many other methods) to characterise interarea oscillations, both in perturbed conditions and during normal operating conditions (i.e., in the absence of significant oscillations). The qualitative conclusions of Terna implementation and experience over many years on some of them is summarized in Table 3.

Table 3 *Pros and cons of different approaches.*

	Accuracy	*Computational time*	*Robustness*	*Complexity*
DMD	+++	+++	+++	-
PCA	++	++	++	--
FDD	+++	+	++	---

In general, the DMD was found less requiring in terms of computation time, more robust and without any particular complexity.

In this section, some selected results of the above methods are shown, with reference to a significant oscillatory event in Europe, occurred on December 3rd, 2017, when an interarea oscillation was detected by different control rooms in Continental Europe. The oscillations lasted approximately 10 minutes at almost 0.29 Hz, leading to think that the north-south mode had been excited. It started at around 1.09 a.m. and reached its maximum deviation around 1.15 a.m., when a dispatch command was implemented to damp it. When the event reached its peak, the southern part of Italy was oscillating against the rest of the Continental European grid with an amplitude of ± 150 mHz, six times larger than oscillation observed in Denmark.

Some frequency measurements of the six buses considered, sampled at 10 Hz for a total of 1200 s, are shown in Fig. 10. Four of them were recorded in Italy, one in Switzerland, one in Denmark.

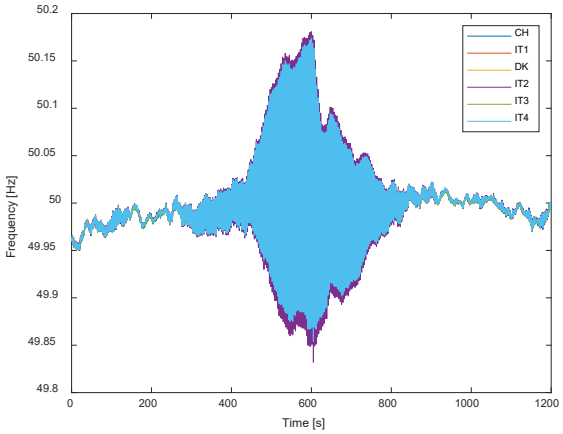

Fig. 10. *Frequency measurements of six PMUs. Data are provided by Terna.*

Since real PMU data may be corrupted by noise or lost due to the communication system, some pre-processing functions are applied for the real-time application. In particular, three steps are carried out:

- *missing data:* interpolation is used to fill possible missing data;
- *data detrend and normalization:* data are detrended and then normalized, as proposed in [31];
- *pass band filtering:* data are filtered by a passband filter with pass-band frequencies set between 0.05 Hz and 2 Hz [32].

In order to set the most suited value of the rank *r*, it is useful to analyse the SVD results (Fig. 11). To better appreciate it, the SVD has been applied to a window of data where the event has already started, between 585 s and 600 s. From the singular values in Fig. 11, it is possible to check that the contribution of singular values above the 5th-6th components is negligible. Hence, the rank for the algorithm has been set to 4 during all the analysis.

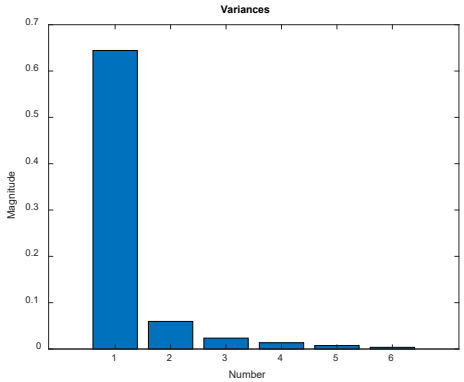

Fig. 11. *Singular values evaluated in the time frame 585-600 s.*

The DMD has been applied to the entire data set and a 15 s sliding window has been adopted. Fig. 12 reports in each plot the frequency, damping and energy, respectively, of the most energetic mode tracked by the DMD: when the event shows up, the energy increases suddenly.

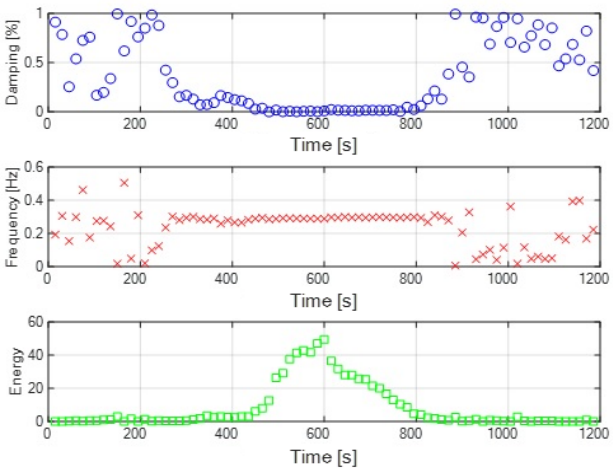

Fig. 12. *Frequency, damping and energy of the most energetic oscillatory mode in each time window considered.*

Ranking the modes according to their energy makes it possible to catch the N-S mode, characterized by an average frequency of 0.2830 Hz and very low (even negative) damping, from the beginning of the phenomenon. Moreover, energy can be used to trigger alarms in the control room based on a threshold.

For each time-window, the mode shapes are computed. Fig. 13 depicts the mode shape considering the time window between 585 and 600 seconds; it indicates that, as expected, the Italian system swings almost in phase with the Central Europe, Switzerland, but in phase opposition with the Northern Europe, Denmark.

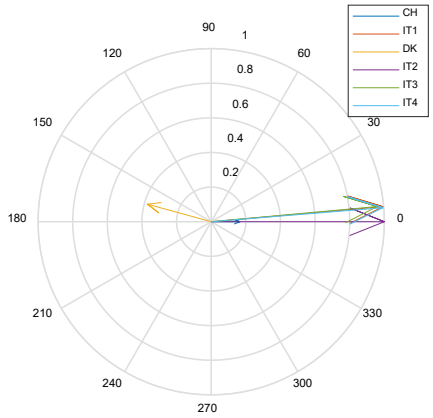

Fig. 13. *Mode shapes estimated into the time interval 585-600 s.*

The power spectrum of the measurements (Fig. 14) depicts a peak at 0.29 Hz, which confirms the DMD findings.

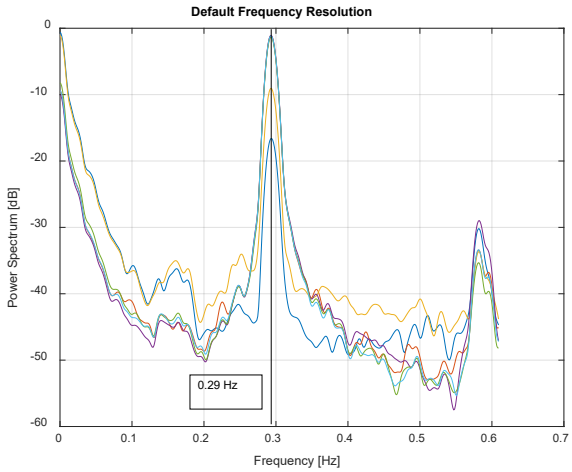

Fig. 14. *Power spectrum.*

Regarding the computation time, a sliding frame 15 s wide (150 samples), using a rank 6 reduction, requires less than 0.1 s, making the proposed algorithm suitable for real-time applications.

The same data have been analysed using the FDD algorithm with the same sliding window (Fig. 15); the identification of both the frequency and the damping is more difficult, as it provides good estimation only between 500 s to 800 s.

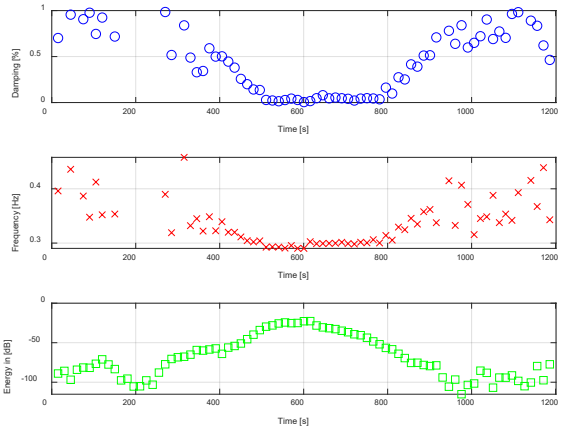

Fig. 15. *Frequency, damping and energy of the most energetic oscillatory mode in each time window considered using the FDD algorithm.*

Finally, data have been analysed also using the PCA combined with Prony algorithm (Fig. 16), confirming again the quality of the DMD results: frequency is estimated with very good accuracy, from the beginning of the event, thus giving a global overview of the grid behaviour; however, this method does not provide information on the mode shapes.

It is worth noticing that the proposed algorithm based on the DMD can provide useful information also in the absence of a particular event: in particular, valuable information can be derived to identify the most important parameters influencing different types of oscillations (e.g., load demand, active power flows through tie-lines, percentage of renewables, import, etc.). At the same time, in

such conditions, the low and quite constant energy trend suggests that no oscillations are taking place.

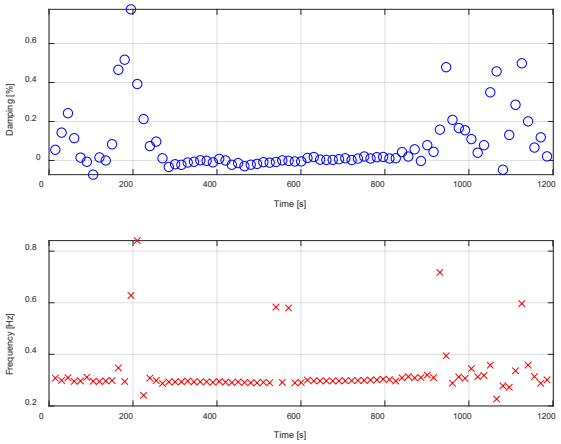

Fig. 16. *Frequency and damping of the first component identified by the PCA/Prony algorithm.*

4. Conclusions

The paper proposes a new approach to the real-time identification of interarea oscillations based on the Dynamic Mode Decomposition. It is based on the latest formulation of this decomposition and it takes advantage of a newly defined energy mode, which enables to track the most significant electromechanical modes in real-time, since they are characterized by the higher energy values, while the numerically transient modes are simply discarded. The proposed method makes it possible for system operators to identify frequency, damping and mode shapes of most significant oscillation modes, and to issue suitable alarms when energy exceeds fixed limits.

Thanks to the tests carried out on both simulated and real-time data, the DMD algorithm has been demonstrated accurate, as compared to linear analysis, and suited for the detection of electromechanical modes in real systems, under noisy and non-stationary conditions. It also gives a quite good representation of the spatial behaviour of the event, through the mode shape plots, that can be computed in times compatible for real-time applications.

Due to its reliability and robustness, the algorithm has been implemented in the control room of Terna, for a real-time monitoring of the grid and, in case of sustained electromechanical oscillations, to issue alarms.

5. References

[1] P. Kundur, N. J. Balu, and M. G. Lauby, *Power system stability and control*. McGraw-Hill, 1994.

[2] L. Dosiek, "The Effects of Forced Oscillation Frequency Estimation Error on the LS-ARMA+S Mode Meter," *IEEE Trans. Power Syst.*, vol. 35, no. 2, pp. 1650–1652, 2020, doi: 10.1109/TPWRS.2020.2965765.

[3] I. Singh *et al.*, "Using Synchrophasor Technology for Monitoring and Analysing Jan 11, 2019 North American Eastern Interconnection System Oscillations," *CIGRE Sess. 48, Pap. C2-105, Paris*, pp. 1–10, 2020.

[4] H. Zhang, P. Zhang, and X. Wang, "Estimation of inter-area modes during ambient operation using the Eigen-system realization algorithm," in *POWERCON 2014 - 2014 International Conference on Power System Technology: Towards Green, Efficient and Smart Power System, Proceedings*, 2014, pp. 569–574, doi: 10.1109/POWERCON.2014.6993769.

[5] X. Li *et al.*, "An eigensystem realization algorithm based data-driven approach for extracting electromechanical oscillation dynamic patterns from synchrophasor measurements in bulk power grids," *Int. J. Electr. Power Energy Syst.*, vol. 116, no. September 2019, p. 105549, 2020, doi: 10.1016/j.ijepes.2019.105549.

[6] M. Netto and L. Mili, "A robust Prony method for power system electromechanical modes identification," in *IEEE Power and Energy Society General Meeting*, 2018, vol. 2018-Janua, pp. 1–5, doi: 10.1109/PESGM.2017.8274323.

[7] J. J. Sanchez-Gasca, *Identification of Electromechanical Modes in Power Systems*, no. June 2012. 2012.

[8] R. B. Leandro, A. S. e Silva, I. C. Decker, and M. N. Agostini, "Identification of the Oscillation Modes of a Large Power System Using Ambient Data," *J. Control. Autom. Electr. Syst.*, vol. 26, no. 4, pp. 441–453, 2015, doi: 10.1007/s40313-015-0187-1.

[9] S. A. Nezam Sarmadi and V. Venkatasubramanian, "Electromechanical Mode Estimation Using Recursive Adaptive Stochastic Subspace Identification," *IEEE Trans. Power Syst.*, vol. 29, no. 1, pp. 349–358, Jan. 2014, doi: 10.1109/TPWRS.2013.2281004.

[10] H. Khalilinia, L. Zhang, and V. Venkatasubramanian, "Fast Frequency-Domain Decomposition for Ambient Oscillation Monitoring," *IEEE Trans. Power Deliv.*, vol. 30, no. 3, pp. 1631–1633, Jun. 2015, doi: 10.1109/TPWRD.2015.2394403.

[11] J. C. H. Peng and N. K. C. Nair, "Enhancing Kalman filter for tracking ringdown electromechanical oscillations," *IEEE Trans. Power Syst.*, vol. 27, no. 2, pp. 1042–1050, May 2012, doi: 10.1109/TPWRS.2011.2169284.

[12] T. A. Papadopoulos, A. I. Chrysochos, E. O. Kontis, and G. K. Papagiannis, "Ringdown analysis of power systems using vector fitting," *Electr. Power Syst. Res.*, vol. 141, pp. 100–103, Dec. 2016, doi: 10.1016/j.epsr.2016.07.016.

[13] X. Wang, J. W. Bialek, and K. Turitsyn, "PMU-Based Estimation of Dynamic State Jacobian Matrix and Dynamic System State Matrix in Ambient Conditions," *IEEE Trans. Power Syst.*, vol. 33, no. 1, pp. 681–690, Jan. 2018, doi: 10.1109/TPWRS.2017.2712762.

[14] D. Lauria and C. Pisani, "On Hilbert transform methods for low frequency oscillations detection," *IET Gener. Transm. Distrib.*, vol. 8, no. 6, pp. 1061–1074, 2014, doi: 10.1049/iet-gtd.2013.0545.

[15] D. Lauria and C. Pisani, "Improved non-linear least squares method for estimating the damping levels of

electromechanical oscillations," *IET Gener. Transm. Distrib.*, vol. 9, no. 1, pp. 1–11, 2015, doi: 10.1049/iet-gtd.2014.0055.

[16] A. Bosisio *et al.*, "Combined use of PCA and Prony Analysis for Electromechanical Oscillation Identification," in *ICCEP 2019 - 7th International Conference on Clean Electrical Power: Renewable Energy Resources Impact*, 2019, pp. 62–70, doi: 10.1109/ICCEP.2019.8890192.

[17] A. K. Gupta, K. Verma, and K. R. Niazi, "Real-time low-frequency oscillations monitoring and coherency determination in a wind-integrated power system," in *Lecture Notes in Electrical Engineering*, 2020, vol. 607, pp. 163–172, doi: 10.1007/978-981-15-0214-9_20.

[18] B. Wang, G. Cai, D. Yang, L. Wang, and Z. Yu, "Investigation on dynamic response of grid-tied VSC during electromechanical oscillations of power systems," *Energies*, vol. 13, no. 1, 2019, doi: 10.3390/en13010094.

[19] D. Yang, B. Wang, G. Cai, and J. Wen, "Oscillation mode analysis for power grids using adaptive local iterative filter decomposition," *Int. J. Electr. Power Energy Syst.*, vol. 92, pp. 25–33, 2017, doi: 10.1016/j.ijepes.2017.04.004.

[20] P. J. Schmid, "Dynamic mode decomposition of numerical and experimental data," *J. Fluid Mech.*, vol. 656, pp. 5–28, 2010, doi: 10.1017/S0022112010001217.

[21] E. Barocio, B. C. Pal, N. F. Thornhill, and A. R. Messina, "A Dynamic Mode Decomposition Framework for Global Power System Oscillation Analysis," *IEEE Trans. Power Syst.*, vol. 30, no. 6, pp. 2902–2912, 2015, doi: 10.1109/TPWRS.2014.2368078.

[22] S. Mohapatra and T. J. Overbye, "Fast modal identification, monitoring, and visualization for large-scale power systems using Dynamic Mode Decomposition," *19th Power Syst. Comput. Conf. PSCC 2016*, pp. 1–7, 2016, doi: 10.1109/PSCC.2016.7540904.

[23] D. Yang, T. Zhang, G. Cai, B. Wang, and Z. Sun, "Synchrophasor-Based Dominant Electromechanical Oscillation Modes Extraction Using OpDMD Considering Measurement Noise," *IEEE Syst. J.*, vol. 13, no. 3, pp. 3185–3193, 2019, doi: 10.1109/JSYST.2019.2900063.

[24] J. H. Tu, C. W. Rowley, D. M. Luchtenburg, S. L. Brunton, and J. N. Kutz, "On dynamic mode decomposition: Theory and applications," *J. Comput. Dyn.*, vol. 1, no. 2, pp. 391–421, 2014, doi: 10.3934/jcd.2014.1.391.

[25] J. Kou and W. Zhang, "An improved criterion to select dominant modes from dynamic mode decomposition," *Eur. J. Mech. B/Fluids*, vol. 62, pp. 109–129, 2017, doi: 10.1016/j.euromechflu.2016.11.015.

[26] J. C. A. Barata and M. S. Hussein, "The Moore-Penrose Pseudoinverse: A Tutorial Review of the Theory," *Brazilian Journal of Physics*, vol. 42, no. 1–2. pp. 146–165, Apr-2012, doi: 10.1007/s13538-011-0052-z.

[27] J. N. Kutz, S. L. Brunton, B. W. Brunton, and J. L. Proctor, *Dynamic Mode Decomposition*. Siam, 2016.

[28] B. O. Koopman, "Hamiltonian Systems and Transformation in Hilbert Space.," *Proc. Natl. Acad. Sci. U. S. A.*, vol. 17, no. 5, pp. 315–8, May 1931, doi: 10.1073/pnas.17.5.315.

[29] D. J. Trudnowski, J. W. Pierre, N. Zhou, J. F. Hauer, and M. Parashar, "Performance of three mode-meter block-processing algorithms for automated dynamic stability assessment," *IEEE Trans. Power Syst.*, vol. 23, no. 2, pp. 680–690, 2008, doi: 10.1109/TPWRS.2008.919415.

[30] G. Rogers, *Power system oscillations*. Kluwer Academic, 2000.

[31] L. Vanfretti, S. Bengtsson, and J. O. Gjerde, "Preprocessing synchronized phasor measurement data for spectral analysis of electromechanical oscillations in the Nordic Grid," *Int. Trans. Electr. Energy Syst.*, vol. 25, no. 2, pp. 348–358, Feb. 2015, doi: 10.1002/etep.1847.

[32] G. D'Antona and A. Ferrero, *Digital signal processing for measurement systems : theory and applications*. Springer, 2006.